ORBITAL PROCESSING OF HIGH-QUALITY CdTe COMPOUND SEMICONDUCTORS

D. J. Larson, Jr.*, J. I. D. Alexander+, D. Gillies^, F. M. Carlson✻, J. Wu✧ and D. Black☆

*Grumman Aerospace Corporation, Bethpage, NY.
+Center for Microgravity and Materials Research, University of Alabama in Huntsville, Huntsville, AL.
^NASA Marshall Space Flight Center, Huntsville, AL.
✻Dept. of Mechanical and Industrial Engineering, Clarkson University, Potsdam, NY.
✧University of New York - Stony Brook, Stony Brook, NY.
☆National Institute of Standards and Technology, Gaithesburg, Washington, D.C.

ABSTRACT

CdZnTe crystals were grown in one-g and in μ-g for comparative analysis. The two μ-g crystals were grown in the Crystal Growth Furnace during the First United States Microgravity Laboratory Mission (USML-1). The samples were analyzed for chemical homogeneity, structural perfection, and opto-electronic performance (infrared transmission).

FTIR transmission of both ground and flight materials showed that the infrared transmission was close to theoretical, 63% versus 66%, suggesting that the material was close to the stoichiometric composition during both the ground and flight experiments. Infrared microscopy confirmed that the principal precipitates were Te and their size (1-10 μm) and density suggested that the primary flight and ground base samples experienced similar cooling rates.

Macrosegregation was predicted, using scaling analysis, to be low even in one-g crystals and this was confirmed experimentally, with nearly diffusion controlled growth achieved even in the partial mixing regime on the ground. Radial segregation was monitored in the flight samples and was found to vary with fraction solidified, but was disturbed due to the asymmetric gravitational and thermal fields experienced by the flight samples.

The flight samples, however, were found to be much higher in structural perfection than the ground samples produced in the same furnace under identical growth conditions except for the gravitational level. Rocking curve widths were found to be substantially reduced, from 20/35 (one-g) to 9/20 (μ-g) for the best regions of the crystals. The FWHM of 9 arc seconds is as good as the best reported terrestrially for this material. The ground samples were found to have a fully developed mosaic structure consisting of subgrains, whereas the flight sample dislocations were discrete and no mosaic

Joint "L+1" Science Review for USML-1 and USMP-1 with the Microgravity Measurement Group, September 22-24, 1993, Huntsville, Alabama, USA.

substructure was evident. The defect density was reduced from 50-100,00 (one-g) to 500-2500 EPD (μ-g). These results were confirmed using rocking curve analysis, synchrotron topography, and etch pit analysis.

The low dislocation density is thought to have resulted from the near-absence of hydrostatic pressure which allowed the melt to solidify with minimum or no wall contact, resulting in very low stress being exerted on the crystal during growth or during post-solidification cooling.

INTRODUCTION

CdZnTe is a technologically important member of the family of II-VI compound semiconductors. The most important application of CdZnTe is as a lattice-matched substrate for the epitaxial growth of HgCdTe infrared detectors. The requirements for large area infrared devices have led to increased reliance on epitaxial processes to provide detector-grade material and a concomitant demand for high quality substrates. These substrates are typically grown using unseeded, modified horizontal and vertical Bridgman crystal growth techniques.

Presently, HgCdTe epilayers are most frequently fabricated using liquid phase epitaxy (LPE). However, to achieve abrupt device/substrate junctions, epitaxial growth of HgCdTe has been driven to lower temperatures, using chemical vapor deposition or molecular beam techniques. These techniques minimize interdiffusion, but they are much more sensitive to wafer quality, particularly at the surface. In addition, fast diffusion of Hg along dislocation cores has resulted in demands for the minimization of extended defects. This requirement has led to a demand for reduced defect densities in the substrates, as these extended defects are likely to project from the wafer surface into the epilayer.

One solution is to lattice-match the substrate and the epitaxial layer at the growth temperature in order to minimize interfacial strains and dislocation generation, propagation, and/or multiplication at the substrate/epilayer interface. The lattice-matched substrate of choice is CdZnTe. The primary needs for these CdZnTe applications are therefore (1) increased structural perfection (reduced defect density) within the bulk crystals and substrates, and (2) more uniform lattice parameters (chemical homogeneity) within the substrates, which better match those of the specific HgCdTe composition at the epitaxial growth temperature.

The program described in this paper was initiated to investigate quantitatively the influences of gravitationally dependent phenomena on the growth and quality of compound semiconductors as a means of improving crystal quality (structural and compositional) and to better understand and control the variables within the production process. The empirical effort entailed the development of a one-g experiment baseline for quantitative comparison with the microgravity results. This empirical effort was supported by the development of high-fidelity process models of heat transfer, fluid flow and solute

redistribution, and thermomechanical stress occurring in the furnace, safety cartridge, ampoule, and sample throughout the melting, solidification, and post-solidification processing.

The models were initially used to predict the impact of process parameter variation (trend analysis), allowing us to design critical one-g growth experiments. Subsequently, as the models were empiricized, correlation and optimization experiments in one-g and in microgravity experiments were conducted. Finally, the models were utilized to assist in the interpretation of the flight results and the quantitative comparison of flight and ground base results.

I. EXPERIMENTAL TECHNIQUE

The samples on USML-1 were processed in the Crystal Growth Furnace (CGF) using the seeded Bridgman-Stockbarger method of crystal growth. Bridgman-Stockbarger crystal growth is accomplished by establishing isothermal hot zone and cold zone temperatures with a uniform thermal gradient in between. The thermal gradient spans the melting point of the material (1095°C). After sample insertion, the furnace's hot and cold zones are ramped to temperature (1175°C and 980°C, respectively), establishing a thermal gradient (30°C/cm) in between and melting the bulk of the sample. The furnace is then programmed to move farther back on the sample, causing the bulk melt to come into contact with the high-quality seed crystal, thus seeding the melt. The seed crystal prescribes the growth orientation of the crystal grown. Having seeded the melt, the furnace translation is reversed and the sample is directionally solidified at a uniform velocity (1.6 mm/hr) by moving the furnace and the thermal gradient over the stationary sample.

The CGF samples were characterized and the results from one-g and μ-g were quantitatively compared with respect to chemical homogeneity and structural quality. These 'internal' results were then quantitatively compared with the best results accomplished terrestrially as an 'external' comparison. The 'external' samples were fabricated using the same growth method and the Grumman Programmable Multi-Zone Furnace (PMZF) operated in a low gradient configuration (<10°C/cm). This PMZF material has been shown in the ARPA Infrared Materials Producibility Program to compare favorably with the best CdZnTe crystals grown terrestrially.

The characterization techniques employed in this study included x-ray double crystal rocking curve (DCRC), x-ray precision lattice parameter (PLP), energy dispersive x-ray analysis (EDX), photoreflectance (PR), synchrotron white beam topography (SWBT), and synchrotron monochromatic beam topography (SMBT). Both SWBT (Ref. 1) and SMBT were performed at the National Synchrotron Light Source (NSLS) at the Brookhaven National Laboratory (BNL). The DCRC and PLP measurements were made at Grumman using Blake Instruments custom systems, with Copper radiation and a spot size of ~1mm^2. The EDX and microprobe measurements were made at the Marshall Space Flight Center.

PR (Ref. 2) was carried out at 300K using a He-Ne laser chopped at 200 Hz, a monochromator resolution of about 25 Angstroms and a typical spot size of ~1mm. The energy gap was determined from a lineshape fit using the low-field approximation (Ref. 3,4); the zinc content (x) in $Cd_{(1x)}Zn_{(x)}Te$ was derived from the "calibration curve" of Ref. 2, assuming a constant energy shift in the curve to account for our use of 300K rather than 77K. For DCRC, PLP, and PR the sample was mounted on a micropositioner stage which allowed manual or automatic scanning over the sample surface. All samples were identically chemomechanically polished using a dilute Br-methanol solution (Ref. 5).

II. EXPERIMENTAL PLAN

A. Ground

Ground-base qualification and developmental tests were conducted in the CGF Ground Control Experiments Laboratory (GCEL) to confirm hardware designs for the sample/ampoule, ampoule/cartridge, and the interfaces between these components and instrumentation within the Sample/Ampoule Cartridge Assembly (SACA). Figure 1 shows the ampoule design and location of the instrumentation thermocouples. In addition, timeline compatibility between the four experiments that were to run in series in the CGF on USML-1 and the flight timeline was confirmed. Lastly, the test results served to empiricize the process models and optimized the processing parameters for the flight experiment.

The final CGF ground sample, grown under the optimized process conditions, duplicated the anticipated flight conditions and served as a 'ground truth' sample for quantitative comparison with the primary flight sample. Since we were fortunate to have the opportunity to conduct a second experiment with the flight back-up (secondary) sample, the 'ground truth' experiment for the secondary sample was conducted post-flight. Analyses of these samples focused on the chemical homogeneity and the structural quality of the crystals.

In addition to the CGF 'internal' baseline, an additional 'external' baseline was established using the Programmable Multi-Zone Furnace at the Grumman Corporate Research Center. This furnace system employed lower thermal gradients (<10°C/cm) and slower heating and cooling rates (1°C/min) in order to minimize the thermo-elastic stresses imposed on the sample during processing. These samples were 38mm in diameter as compared to the CGF samples which measured 15mm in diameter. These results were intended to serve as an external comparative baseline representative of the best CdZnTe produced terrestrially. This material has been shown in the ARPA Infrared Materials Producibility Program to compare favorably with the best CdZnTe crystals grown terrestrially.

B. Flight

The USML-1 Mission was planned to process one primary sample, with a back-up sample in stowage outside of the CGF Furnace. The primary sample was successfully processed and due to the premature termination of one of the other experiments, a second flight experiment was possible, but of shorter duration. The furnace heat-up rate, seeding and thermal equilibration time, temperature profile, and cooling rate were identical for both experiments; the primary difference being the duration of the experiments. Since the samples were of identical lengths, this meant that the secondary sample was furnace cooled prior to the completion of solidification of the sample, and a substantial amount of material was solidified under non-plane-front growth conditions. The secondary sample served to confirm the successful seeding technique and to provide additional material from the shouldering region that solidified without wall contact.

Conducting the second experiment demanded unprecedented actions on the part of the crew, particularly: Payload Specialist Eugene Trinh to install the flexible glove box on the CGF, which enabled the processed SACAs to be removed from the CGF; Alternate Payload Specialist Al Sacco to develop the SACA exchange procedures; and Payload Commander Bonnie Dunbar and Pilot Ken Bowersox who exchanged the SACAs, demonstrating for the first time in the US program the ability to exchange potentially toxic materials in the closed environment of the Spacelab. These actions proved the feasibility of conducting similar necessary operations on Space Station, greatly increasing the productivity.

III. EXPERIMENT RESULTS

The Temperature/Time/Position history of the optimized ground experiment is shown as Figure 2. The heat-up rate (2°C/min), thermal equilibration time (2 hrs), solidification velocity (1.6 mm/hr), applied thermal gradient (33 °C/cm) and cool-down rates (2 °C/min) were determined to give the best quality crystals that were consistent with the available flight time and the performance characteristics of the CGF. A ground sample with good crystallinity, grown on the Grumman PMZF in the NASA flight geometry, is shown as Figure 3. This sample is dominated by a large single crystal with a localized twin and a secondary grain nucleated late in the growth process.

The scaling analysis done by Alexander et al (Ref. 7) suggested that the macrosegregation in this system should be relatively low, even in one-g. Chemical mapping of the one-g samples using EDX, microprobe, PR and PLP measurements confirmed this prediction. A typical fit is shown as Figure 4. The shape of the curve suggests that fluid flow is relatively benign and transport is close to diffusion controlled growth, even though still within the partial mixing regime in one-g. The emphasis in analyzing the chemical homogeneity of the flight samples was thus be placed on evaluation of the radial

segregation, since diffusion controlled growth was anticipated. The PMZF 38 mm diameter samples exhibited a solute redistribution coefficient K_e of 1.10, as compared to the equilibrium redistribution coefficient of 1.22. This strongly suggested that the partial mixing in the melt was benign and that diffusion controlled growth could be approached on the ground in large diameter ingots solidified under optimized thermal control longitudinally and radially.

Electro-optical analysis of the CGF ground-base samples indicated that the FTIR transmission was approximately 63% and uniform from 2.5 to 25 microns. This is quite good, as theoretical transmission is approximately 66%. The PMZF material, approached 66%. The flight material was found to be almost identical to the CGF ground material.

Structural analysis indicated that the sample morphology consisted of a mosaic of cells defined by subgrains. Typical rocking curve widths varied systematically from 20 to 35 arc seconds, full width half maximum (FWHM), with the maximum widths at the periphery of the wafer, the minimum midway between the center and the periphery, and the expected 'W' shape from edge to edge.

The Temperature/Time/Position history of the primary flight sample is shown as Figure 5. The major differences between the flight samples and those processed identically on the ground was a measurable difference in the amount of heat flux due to gravitational 'draining' of the liquid volume toward the seed crystal as the sample melted. No thermal surge in temperature at the seed crystal was noted in the flight experiments, suggesting that the transport of the bulk liquid toward the seed was slower and that less fluid volume was transported.

The processed flight ampoules are shown in Figure 6, and radiographs of the interior of the flight ampoules are shown in Figures 7a (primary sample, GCRC-1) and 7b (secondary sample, GCRC-2). It should be noted that the separate bulk liquid was brought in contact with the seed crystal due to the residual gravitational vector, and since the liquid will always wet it's own solid, the seeding operation was successful in both instances.

Careful inspection of the radiographs in Figures 7 shows that both of the crystals grown are separated from the ampoule wall in the shoulder region. This was anticipated and is referred to as 'dewetting', though this term is not strictly correct. Wall contact is not reestablished until the full ampoule cross-section is reached in the steady state region of growth.

It was anticipated that the residual g-vector pointed down the axis of the CGF would result in a thermally and gravitationally symmetric geometry that was thermally stabilizing for our experiment. The orientation of the calculated residual g-vector relative to the Spacelab and the CGF is shown in Figure 8 (Ref. 7). Inspection of the flight samples suggested that this was not correct in the actual experiment. Figure 9 shows the actual primary flight sample after sand blasting the surface. It may be seen that the

sample has a high degree of crystallinity, with a bubble at the top of the shoulder which initiated a twin, and porosity later in the experiment when the sample was furnace cooled.

Analysis of the acceleration data from the mission suggested that there was an unanticipated gravitational component that resulted in gravitational asymmetry at the CGF location (Ref. 7). This was due to the operation of the Shuttle Flash Evaporator System (FES), which operated on approximately a 28 hour cycle (14 hours on and 14 hours off). Figures 10a and 10b show the average orientation of the residual acceleration vector when FES was on, recorded by (a) OARE at the OARE location and extrapolated to the CGF location and (b) PAS on the Flight Deck and extrapolated to the CGF location. It is clear that this is significantly asymmetric relative to the CGF furnace bore axis and could result in thermal and gravitational asymmetry in the flight samples.

The color pattern and surface texture pattern on the surface of the GCRC-1 flight sample, shown in Figures 11 (prior to sand blasting the surface), suggest that each sample solidified without wall contact throughout the shoulder and that when wall contact was resumed, it was only on one side of the ampoule. Partial wall contact would be expected to result from gravitational asymmetry, which was not anticipated and would be expected to cause significant disturbance thermally, possibly solutally, and possibly mechanically because of the absence of hoop stresses during cooling on the free surface side of the sample.

Examination of the surface topography of the primary flight sample, Figure 11a, shows that the areas in full contact with the ampoule wall mirror the surface topography of the wall and appear visually to be very bright surfaces. The topography of the free surfaces shows some thermal etching, but is relatively smooth and has the blue-grey appearance of most semiconductors. The region of partial wall contact, however, is a highly textured matte finish. The surface was found to be comprised of a honeycomb of interconnected hexagonal cells that are nearly perfect hexagons nearest the region of full wall contact and which get progressively more elongated circumferentially as the liquid moves away from the wall. This pattern of contact is shown in Figure 11(b).

Synchrotron White Beam Topography was used to evaluate the surface condition of the flight samples in the three regions of varying wall contact. The regions of total wall contact gave very poor topographic images (not shown), suggesting high levels of surface strain. The regions of no wall contact, however, gave high quality topographs which suggested that the residual strain levels were very low and images of the defect structure suggested the possibility that the defect density was low and that dislocations present were discrete rather than in a fine subgrain or mosaic structure. The regions of no wall contact showed no sign of twinning at the surface. The regions of partial contact, however, showed strong evidence of cross slip, and occasional twinning. Deformation of this type was restricted to the regions of partial wall contact and suggested that the honeycomb surface structure may have acted as a

series of stiction points for the solidification interface resulting in much higher local stresses and concomitant plastic deformation by dislocation and twinning mechanisms.

A topograph of a region of the primary sample that solidified with no wall contact is shown as Figure 12a and a region of the same sample solidified with partial wall contact is shown as Figure 12b. Note the discrete dislocation pattern and low dislocation density in 12a and the high density of dislocations manifested as occasional twinning and extensive slip and in 12b.

Having thoroughly analyzed the surfaces of the samples, the crystals were then oriented using x-ray techniques and wafered such that the wafer surfaces were {111} planes, which is the industry standard. The sectioning plan for the secondary flight sample, which was cropped to remove the portion of the sample that was not plane-front solidified, is shown schematically in Figure 13. The primary sample was sectioned on a {111} plane that was closer to the growth axis of the crystal. The series of real wafers is shown in Figure 14a and the etched wafer surfaces are shown as Figure 14b. The wafers were etched with a lactic acid etchant that differentiates between the A and B faces; A (Cd, Zn) appearing dark and B (Te) appearing light. X-ray synchrotron Bragg reflection topography confirmed that the sample surfaces are entirely {111}, however, there is 180° rotational twinning such that the left third of the wafers are predominantly A faces whereas the remaining portion consists of a single B face. The left side experienced wall contact whereas the right did not. The flight samples were analyzed using DCRC mapping as a measure of residual strain in the crystal. The results suggest that the quality of the flight material, as judged by the full width half maximum (FWHM) of the {333} Bragg diffraction peak, is substantially better than that recorded for the ground truth samples. Area maps of the FWHM for flight wafer 7 is shown as Figure 15. It should be noted that appreciable areas of the flight samples average FWHM values between 10 and 15 arc-seconds, whereas the same regions in the ground truth samples averaged 20 to 35 arc seconds. The strain in the best regions of the flight samples, as indicated by the FWHM of the {333] rocking curve is as low as 9.2 arc seconds. This is fully comparable to the best material that has been grown on the ground using the PMZF technology or any other commercial technology.

The peak distributions are also much different in that the best material is found close to the sample periphery whereas the ground samples evidenced maximum strain and peak width at the periphery. This suggests that unlike the ground samples that were forced to be in mechanical contact with the ampoule walls during processing, the flight samples were not, with a resultant significant reduction in strain. Post flight modeling of this process confirms this suggestion, with the stress experienced by the free surface significantly lower than that at the wall. This is shown in Figure 16.

A further difference between the flight samples and the ground base samples appears in the shape of the DCRC peaks. Figure 17a shows a typical DCRC peak and Gaussian fit for a good region of

a ground sample. The FWHM is about 20 arc-seconds and the fit at the base of the peak, the 'tail' of the curve, is quite poor. This indicates that agreement between diffraction theory and real diffraction is not good. This deviation occurs because the 'tails' of the curve represent the defect structure of the real samples and the defect distribution in these samples is not the ideal distribution that the theory assumes. Figure 17b shows the same peak and fit, except that it is plotted on a log plot which emphasizes the tails of the curve and focuses attention on the lack of agreement between theory and practice. Figure 18 is a ground sample from a complementary study, where the tails of the curve are well described by kinematic diffraction theory. This sample region had a well developed mosaic substructure that conforms well to the description of an 'ideally imperfect' crystal. Figure 19 shows a typical {333} rocking curve peak from a low strain region of the flight material. In this case the tails of the curve are very well described by the Gaussian fit and, taken in concert with the low density discrete dislocation regions imaged on the flight sample surfaces (see Figure 12a), suggested the possibility that this material was 'ideally perfect' material rather than the aforementioned 'ideally imperfect' material which we commonly encounter.

The critical test for this hypothesis was to image the samples topographically in transmission, so that the dislocation structure is imaged directly. Samples of the flight and ground-base materials were chemo-mechanically polished to ≤180μm in thickness and were exposed to monochromatic synchrotron radiation. Only the flight sample could be brought into diffraction; insufficient transmission resulting in no topographic imaging for the ground samples. This suggested the possibility that the higher strain content of the ground samples prevented sufficient transmission whereas the flight sample permitted transmission due to greater crystalline perfection and lower strain. Figure 20 shows the result of this test and clearly shows that the dislocations are low in density and are discrete over large (relative) areas. The singular bright spots are thought to be Te precipitates and the two long straight lines are two variants of {111}[110] twins. This micrograph confirms the discrete nature of the dislocations in the flight material and subsequent dislocation etching of this surface suggested that the dislocation density of this material varied between 500 and 2500 EPD with no mosaic substructure whereas the ground truth material was typically 50,000 to 100,000 EPD and the dislocations formed a continuous mosaic structure.

CONCLUSIONS

FTIR transmission of both ground and flight materials showed that the infrared transmission was close to theoretical, 63% versus 66%, suggesting that the crystals grown were close to the stoichiometric composition in both the ground and flight experiments. Infrared microscopy confirmed that the principal precipitates were Te and their size (<1-10 μm) and density suggested that the primary flight and ground-base samples experienced similar cooling rates and were similar in composition.

Macrosegregation was predicted, using scaling analysis, to be low even in one-g crystals and this was confirmed experimentally. Nearly diffusion controlled growth was achieved even in the partial mixing regime on the ground. Radial segregation was monitored in the flight samples and was found to vary with fraction solidified, but was disturbed due to the asymmetric gravitational and thermal fields experienced by the flight samples.

The flight samples were found to be much higher in structural perfection than the ground samples produced in the same furnace under identical growth conditions except for the gravitational level. The flight material was properly described as 'ideally perfect' material from a diffraction standpoint, whereas ground material was described as ideally imperfect material. The rocking curve width of the best flight material matched the best achieved terrestrially, 9.2 arc-seconds, using any growth technique. The dislocation density was reduced from 50-100,000 in the ground samples, to 500-2500 in the flight samples. The low dislocation density completely eliminated the dislocation substructure that is typical of all ground material. The dislocation reduction is thought to have resulted from the near-absence of hydrostatic pressure in μ-g, which allowed the melt to solidify with minimum or no wall contact, resulting in very low stress being exerted on the crystal during growth and during post-solidification cooling.

ACKNOWLEDGMENTS

We gratefully acknowledge financial support under NASA Contract NAS8-38147. Further, we acknowledge the following Grumman personnel: Andre Berghmans, Frank Chin, and Nils Fonneland, who rendered valuable assistance in growing and characterizing the CdZnTe crystals. We also thank Dr. Louis Casagrande for valuable advice on polishing the wafers and Dr. Donald DiMarzio for assistance in making x-ray measurements. We would also like to acknowledge the technical contributions and generosity of Dr. Michael Dudley, and Dr. Bruce Steiner in conducting synchrotron topography studies.

REFERENCES

1. J. Miltat and Dudley, Chapter 3 in "Applications of Synchrotron Radiation," C. R. A. Catlow and G. N. Greaves (Eds), Blackie and Son Ltd, Glasgow, UK, 65-99, (1990).

2. J. J. Kennedy, P. Amirtharaj, Boyd, Qadri, R. C. Dobbyn, and G. Long, J. Cryst. Growth, v. 86, 93, (1988).

3. D. E. Aspnes, Surf. Sci. v.37, 418, (1973).

4. F. H. Pollak and H. Shen, J. Electronic Materials, v.19 (5), 399, (1990).

5. L. G. Casagrande, D. DiMarzio, M. B. Lee, D. J. Larson, Jr., M. Dudley, and T. Fanning, submitted to the J. Crystal Growth, (1992).

6. C. Parfeniuk, F. Weinberg, I. V. Samarasekera, C. Schvezov, and L. Li, J. Cryst. Growth, v. 119, 261, (1992).

7. J. I. D. Alexander, Orbital Processing of High Quality CdTe Compound Semiconductors: Numerical Modeling and Acceleration Data Analysis, Final Report on Contract Number PO 21-69118, CMMR, University of Alabama in Huntsville, March, 1994.

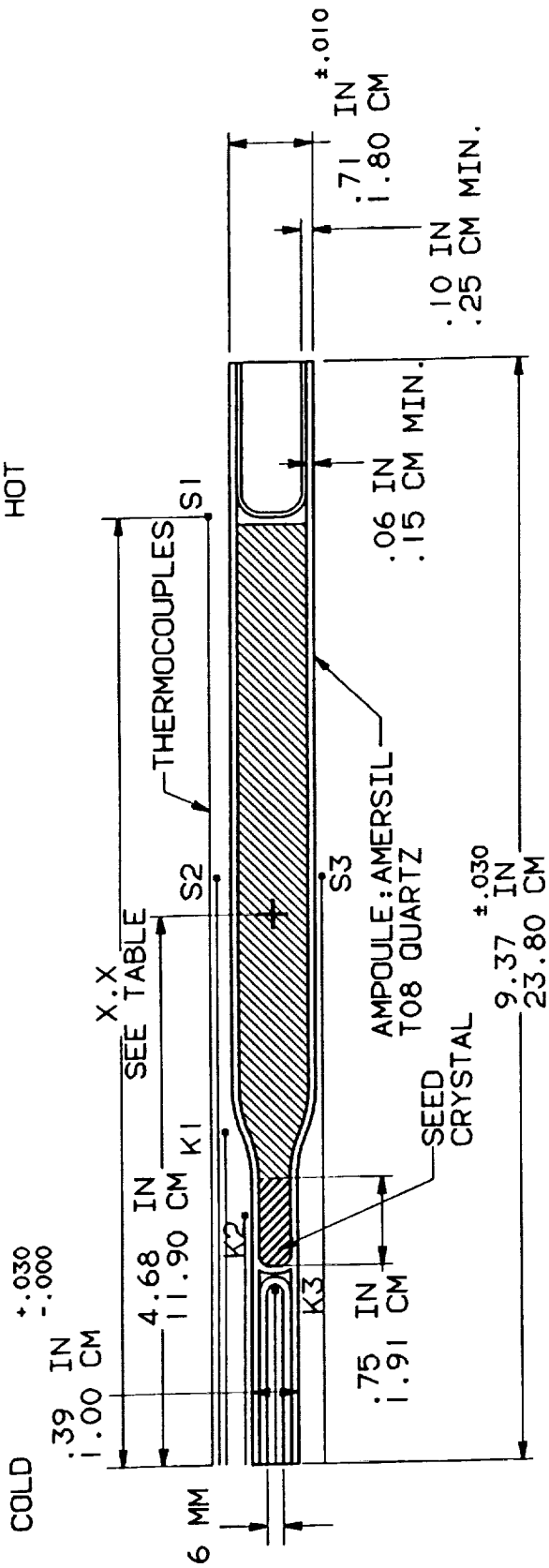

Figure 1 Ampoule Design (Schematic) with Instrumentation Thermocouples.

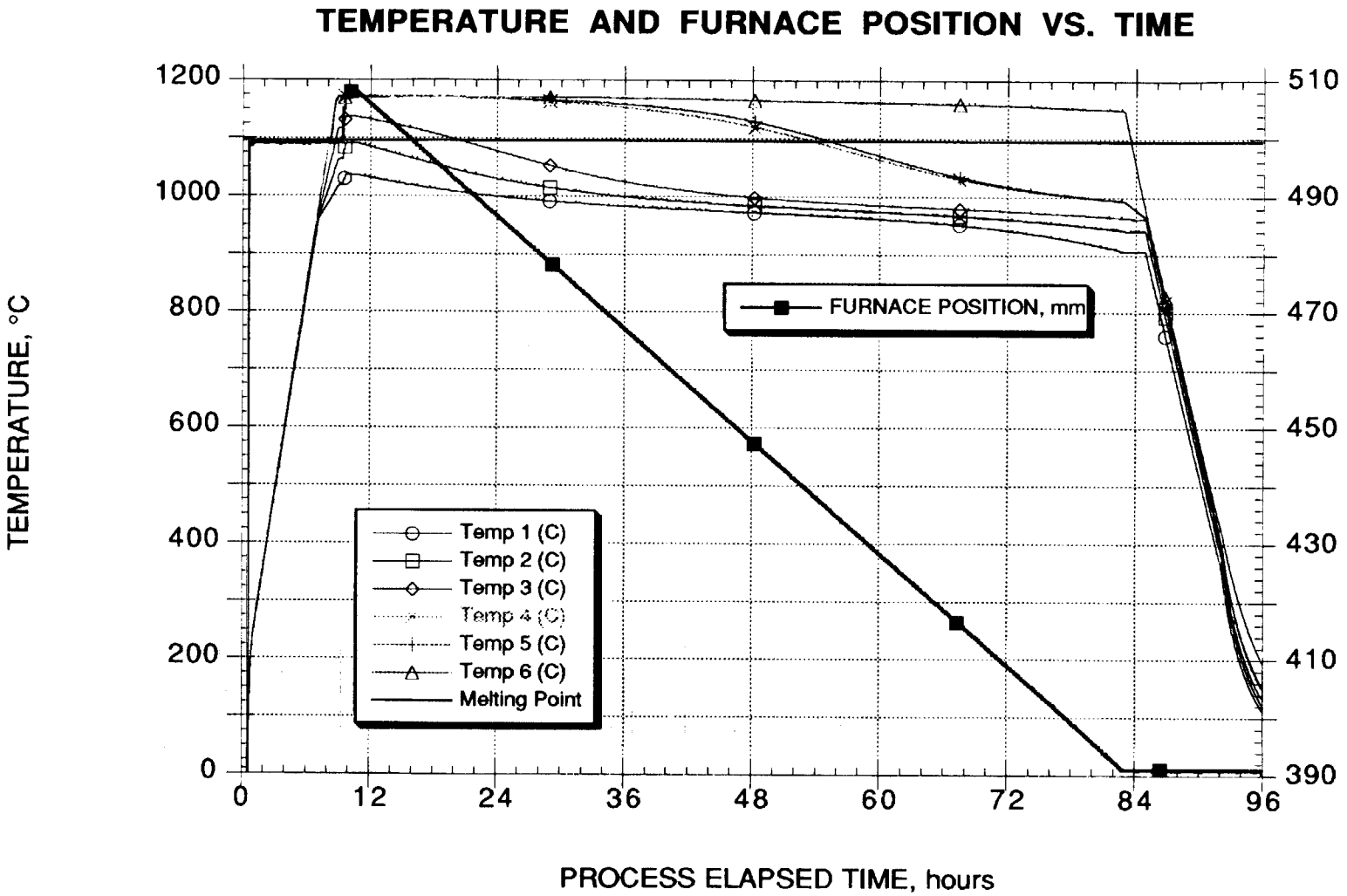

Figure 2 Primary Ground Truth Sample Temperature/Time/Distance History.

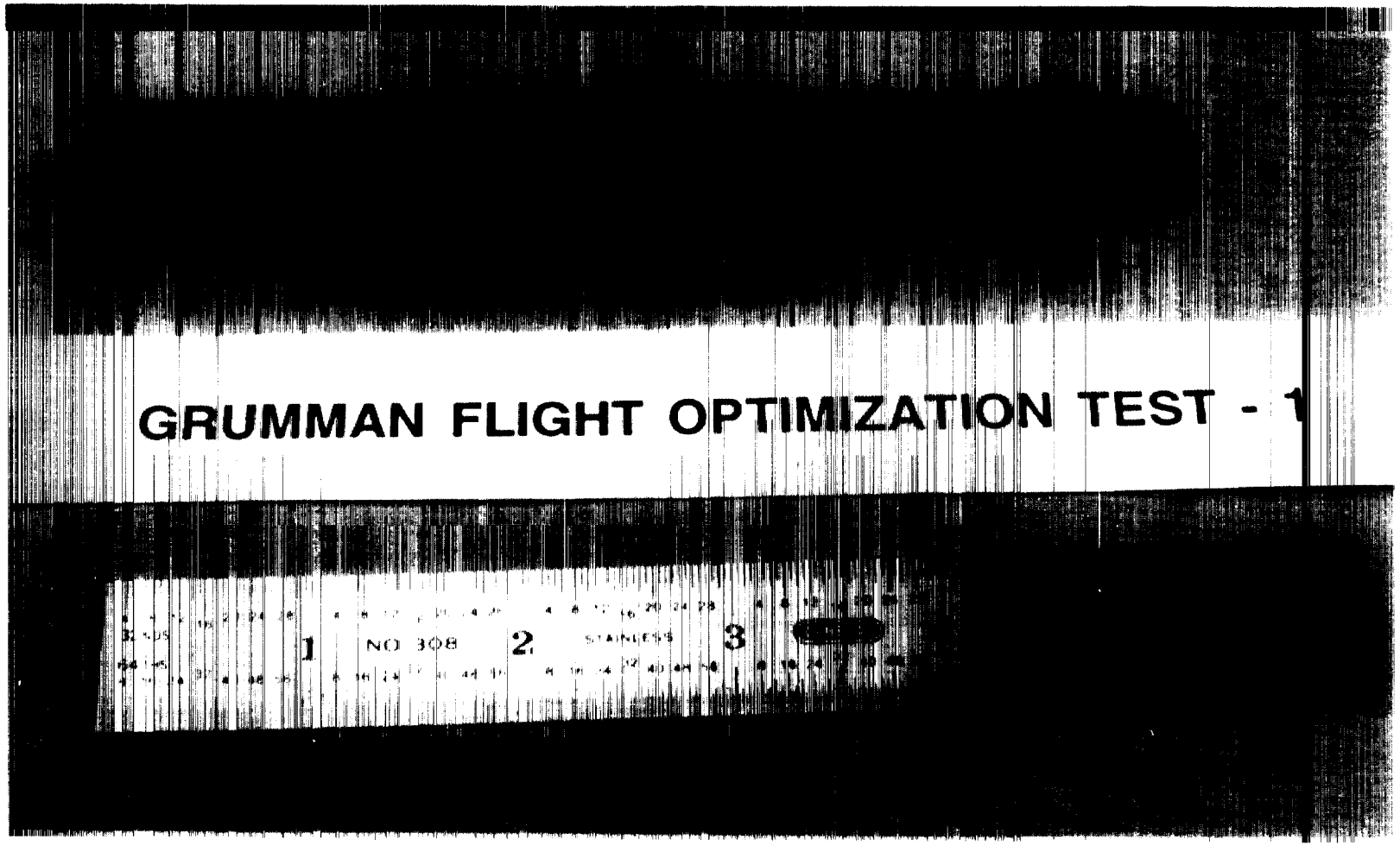

Figure 3 Ground Sample Grown in Grumman PMZF Showing a Dominant Single Crystal Grain.

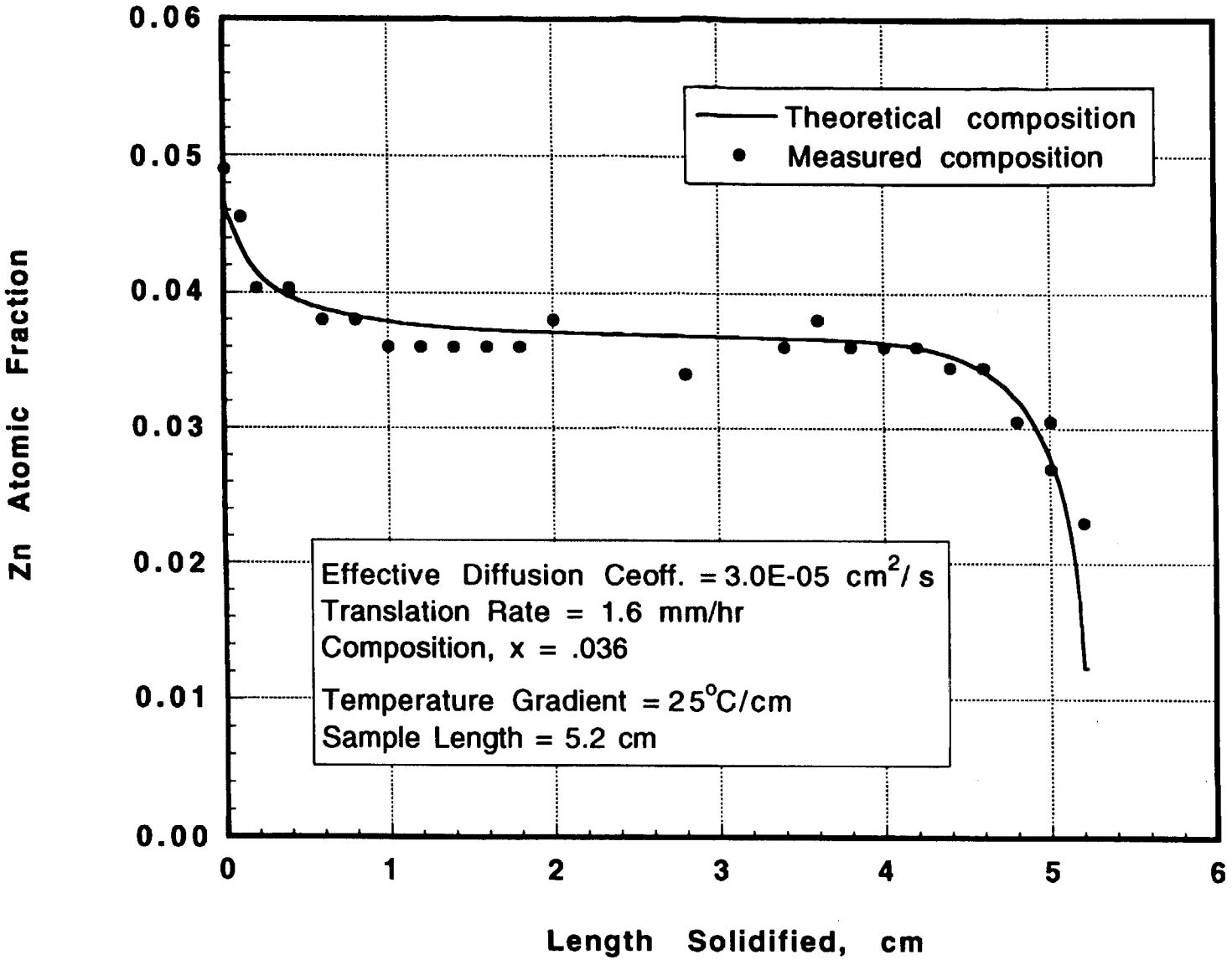

Figure 4 Composition versus Length Solidified, with Calculated Solute Redistribution and Fitting Parameters Superimposed.

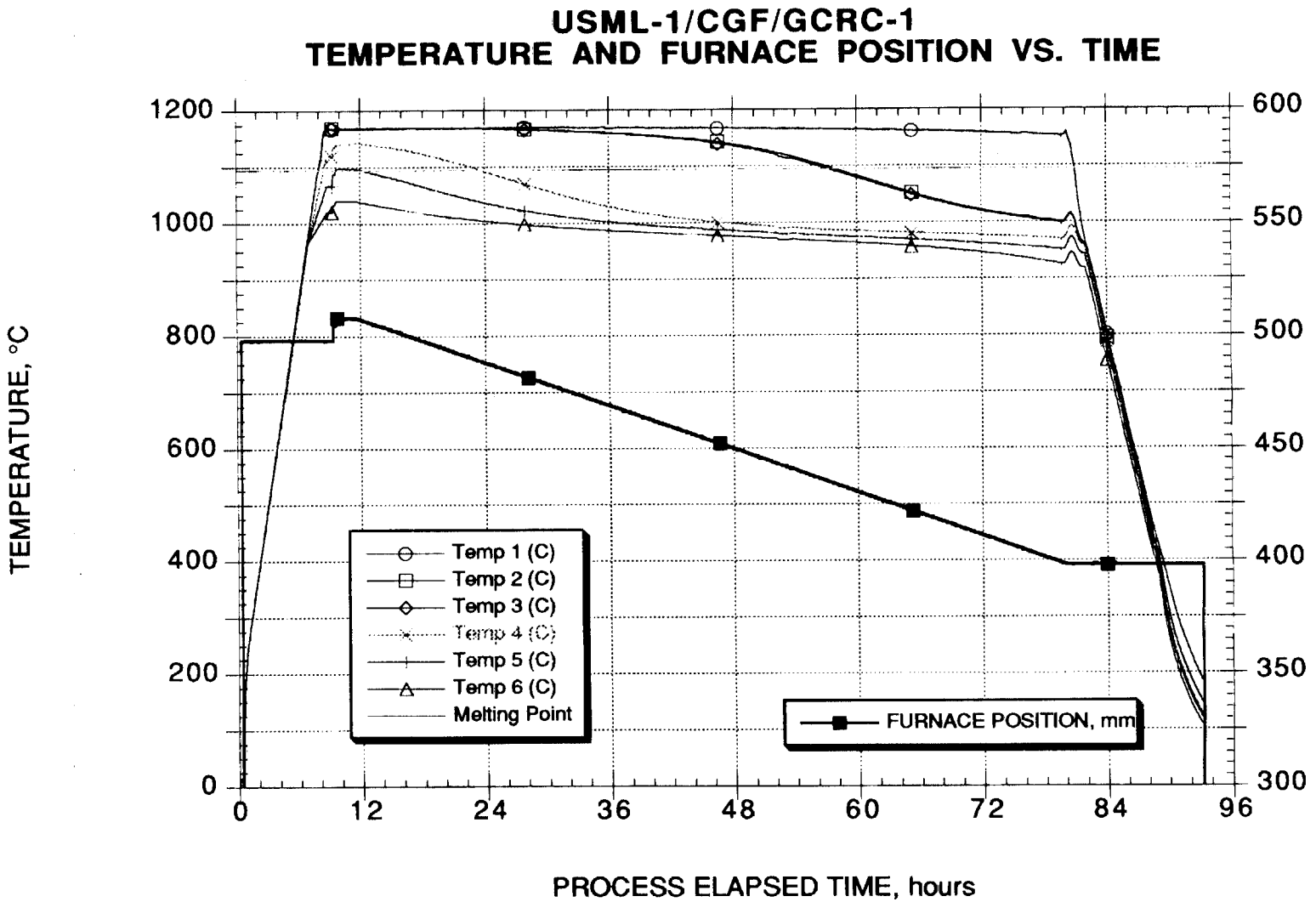

Figure 5 Time/Temperature/Distance History of the Primary Flight Sample, GCRC-1.

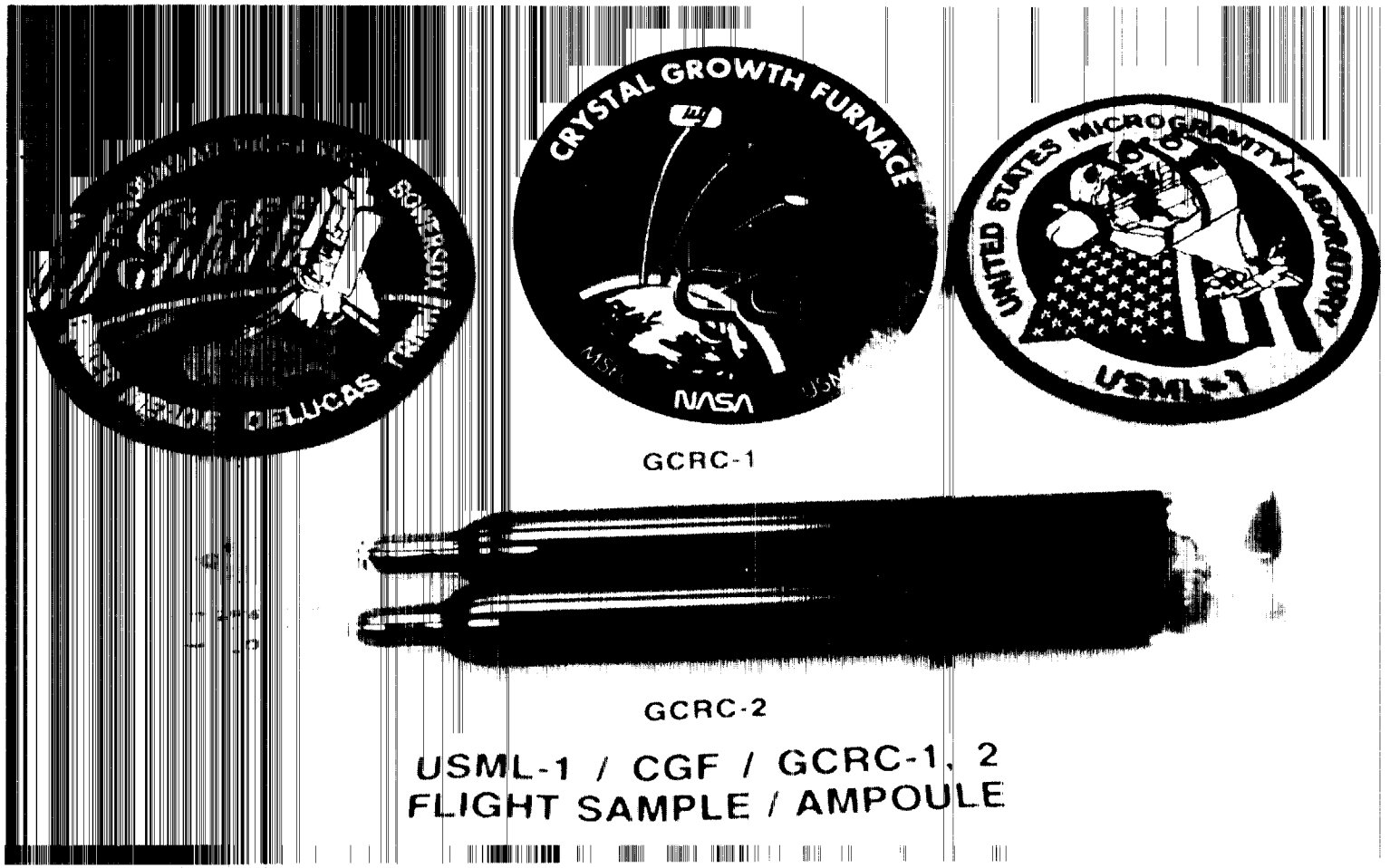

Figure 6 Photograph of Primary and Secondary Flight Ampoules (Post-flight).

(a)

(b)

Figure 7 Post-flight X-Radiographs of (a) the Primary Flight Sample, GCRC-1 Ampoule and (b) the Secondary Flight Sample and Ampoule.

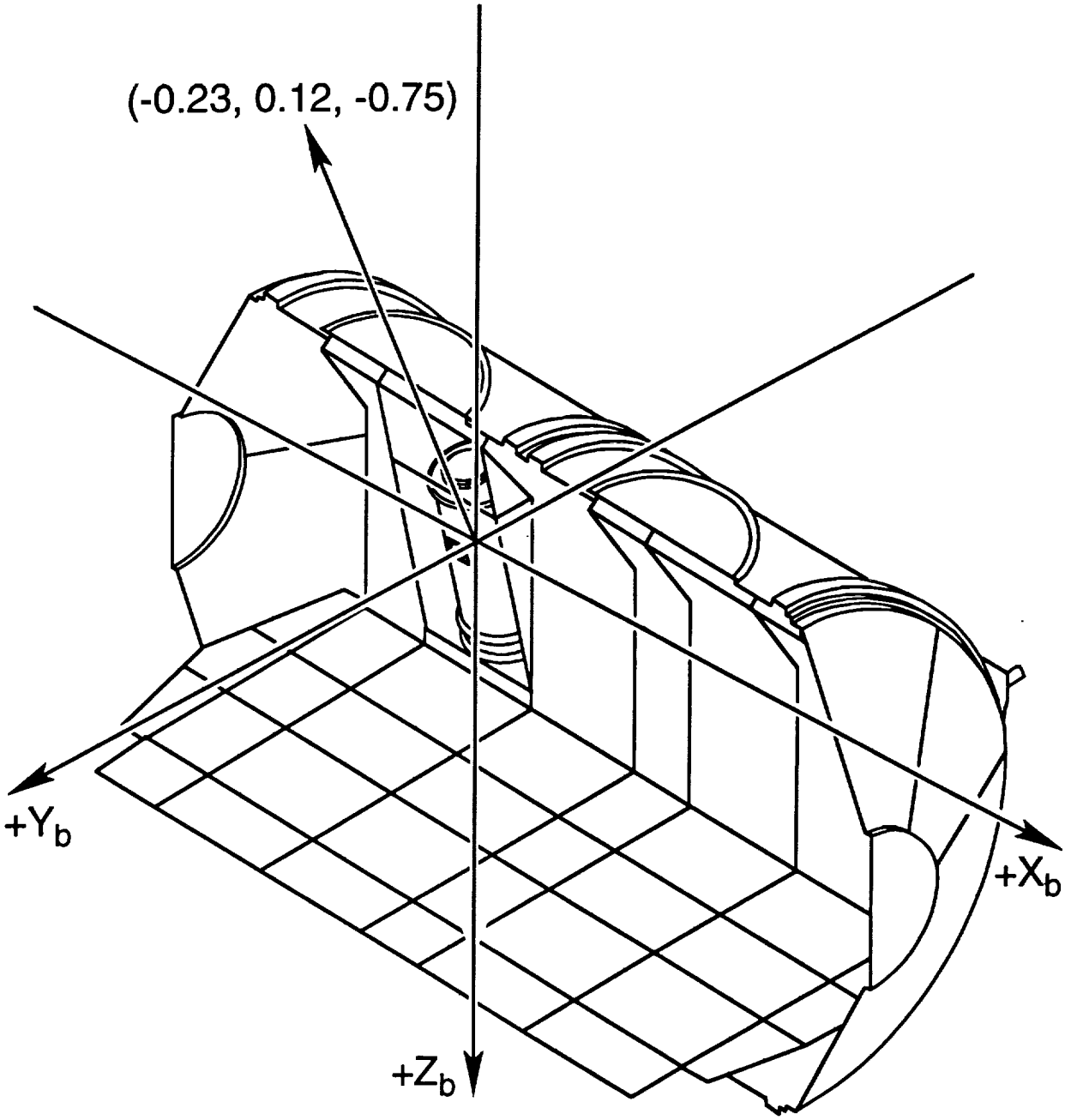

Figure 8 Calculated g-Vector at the CGF location, Without the Flash Evaporator System, (Ref. 7).

Figure 9 Photograph of the Primary Flight Sample, GCRC-1.

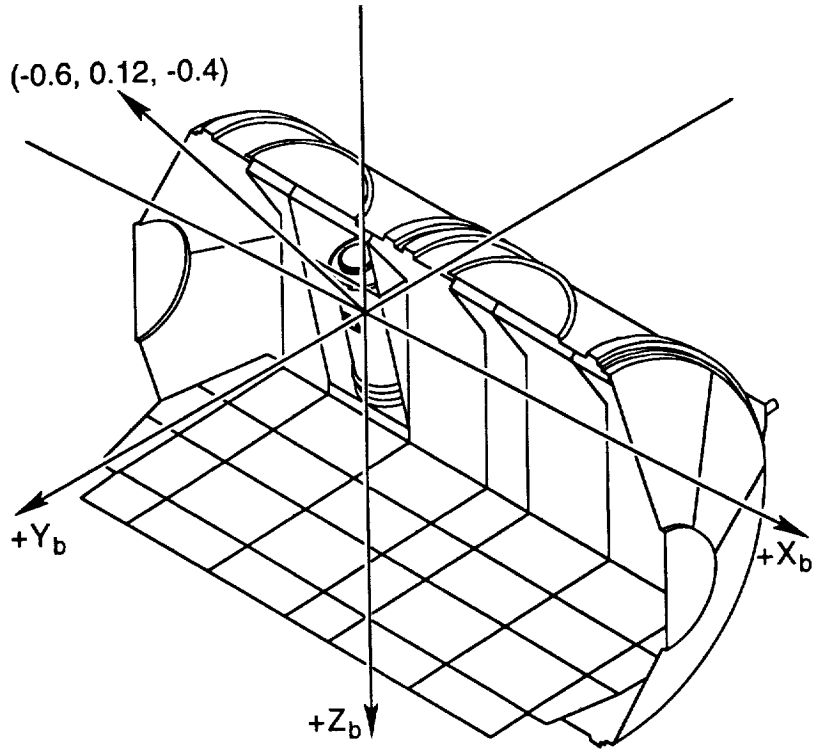

Figure 10a G-Vector at the CGF Location, Calculated from OARE Data.

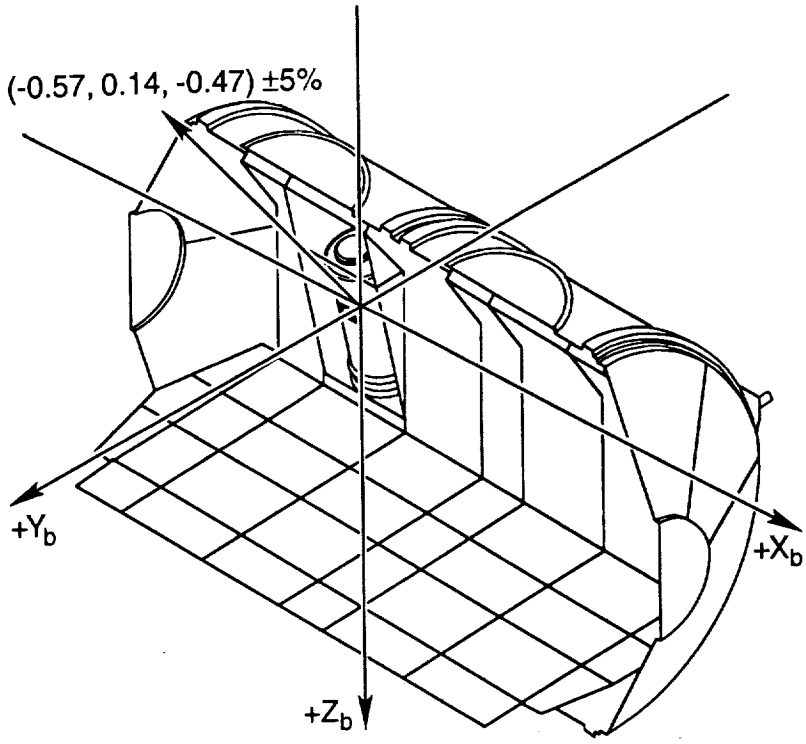

Figure 10b G-Vector at the CGF Location, Calculated from PAS Data.

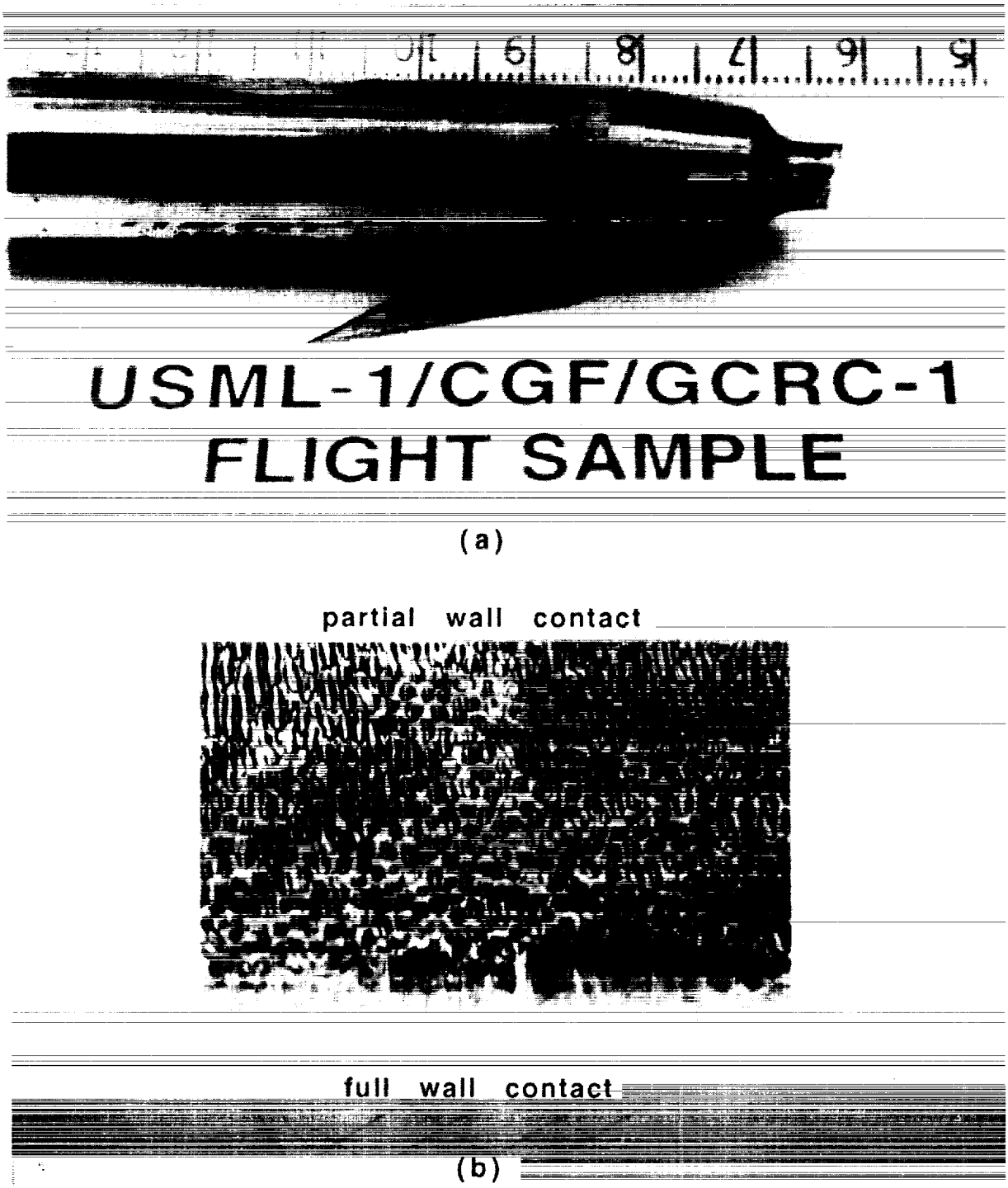

Figure 11 Surface Texture on the GCRC-1 Flight Sample, (a) Seed/Shoulder/Steady State Transition, and (b) Partial Contact Region Showing 'Honeycomb' Surface Structure.

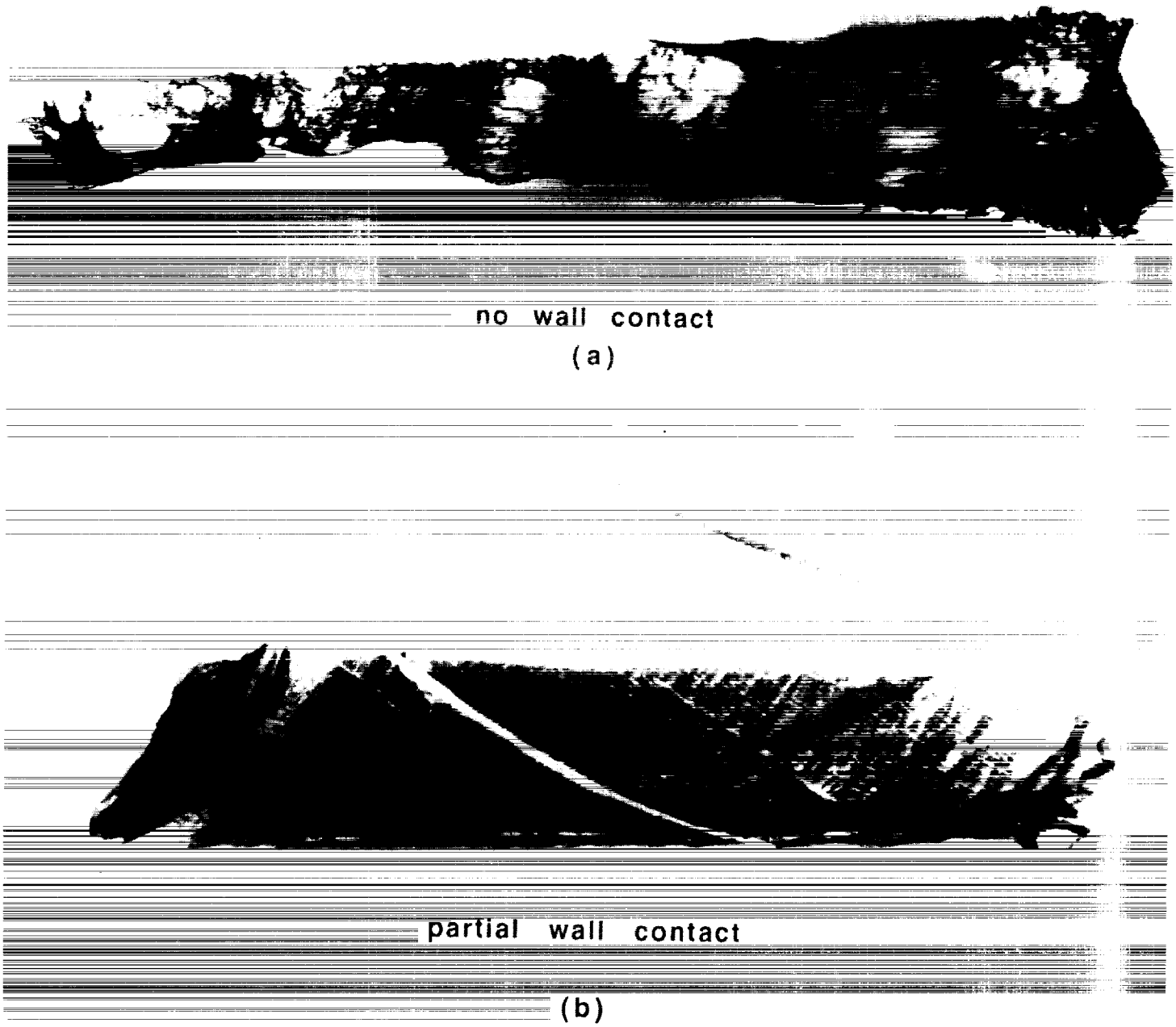

Figure 12 Synchrotron White Beam Topographs of the GCRC-1 Flight Sample Surfaces, a) Region Solidified Without Wall Contact Showing Discrete Dislocations, and b) Partial Contact Region Showing Slip and Twinning.

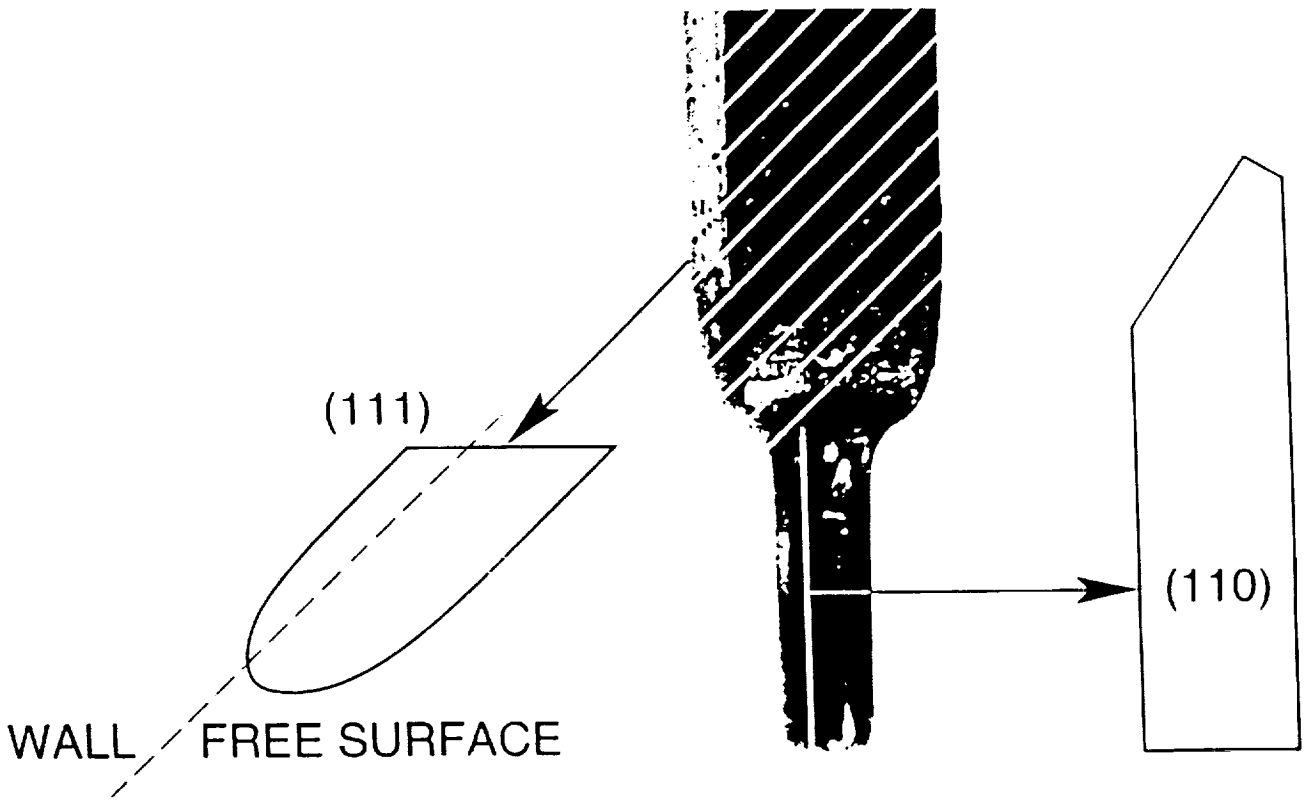

Figure 13 Wafer Sectioning Plan for the Secondary Flight Sample Boule and Seed (Schematic).

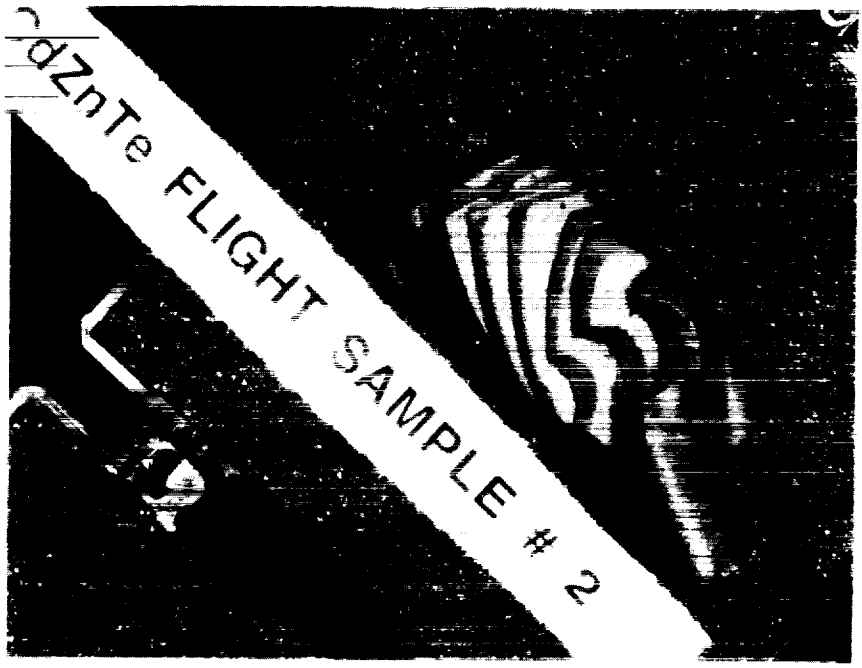

(a)

(b)

Figure 14 {111} Wafer Set Cut from the Secondary Flight Sample, GCRC-2, a) As Cut, and b) Polished/Etched.

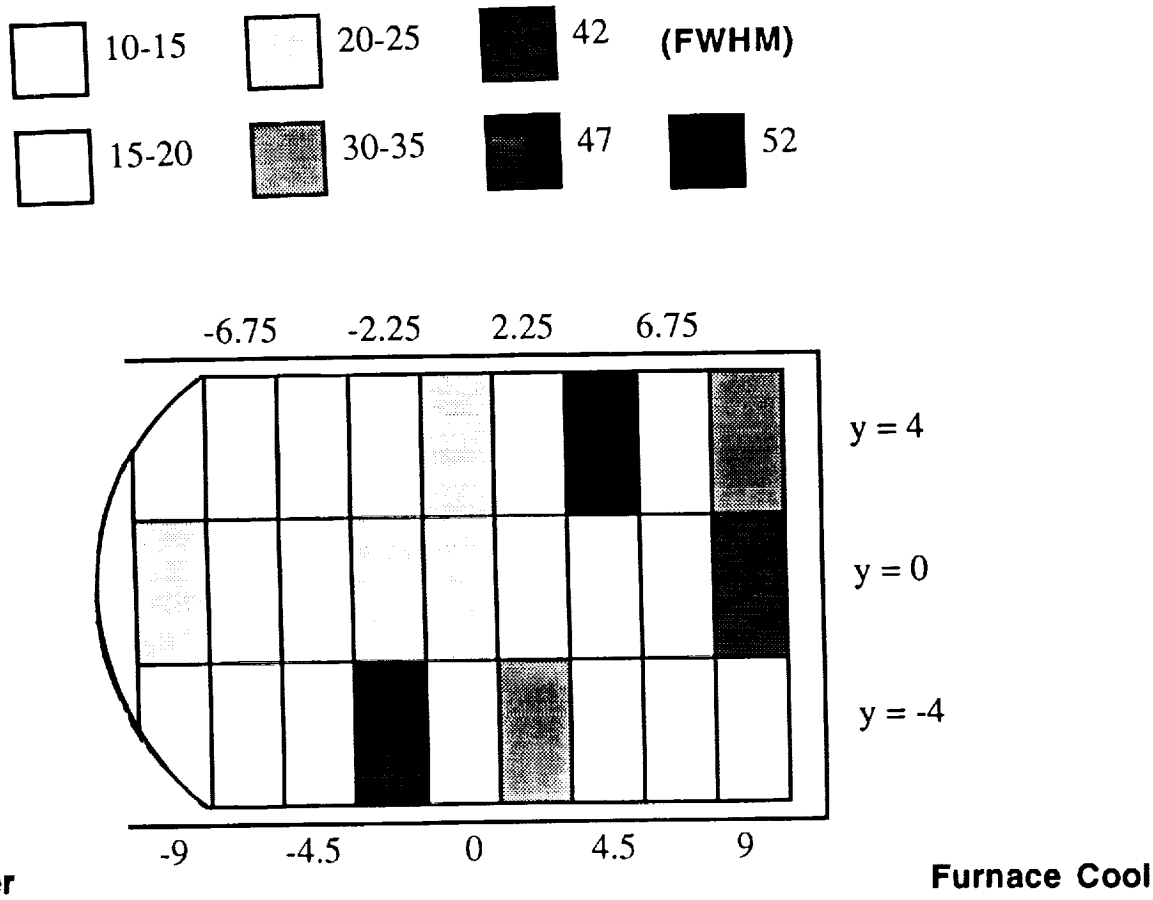

Figure 15 X-Ray Rocking Curve Map (FWHM Vs Position) for GCRC-2 Wafer 7. The Highest Strain Regions do not Originate at the Periphery and the Best Material Coincides with the Regions of No Wall Contact.

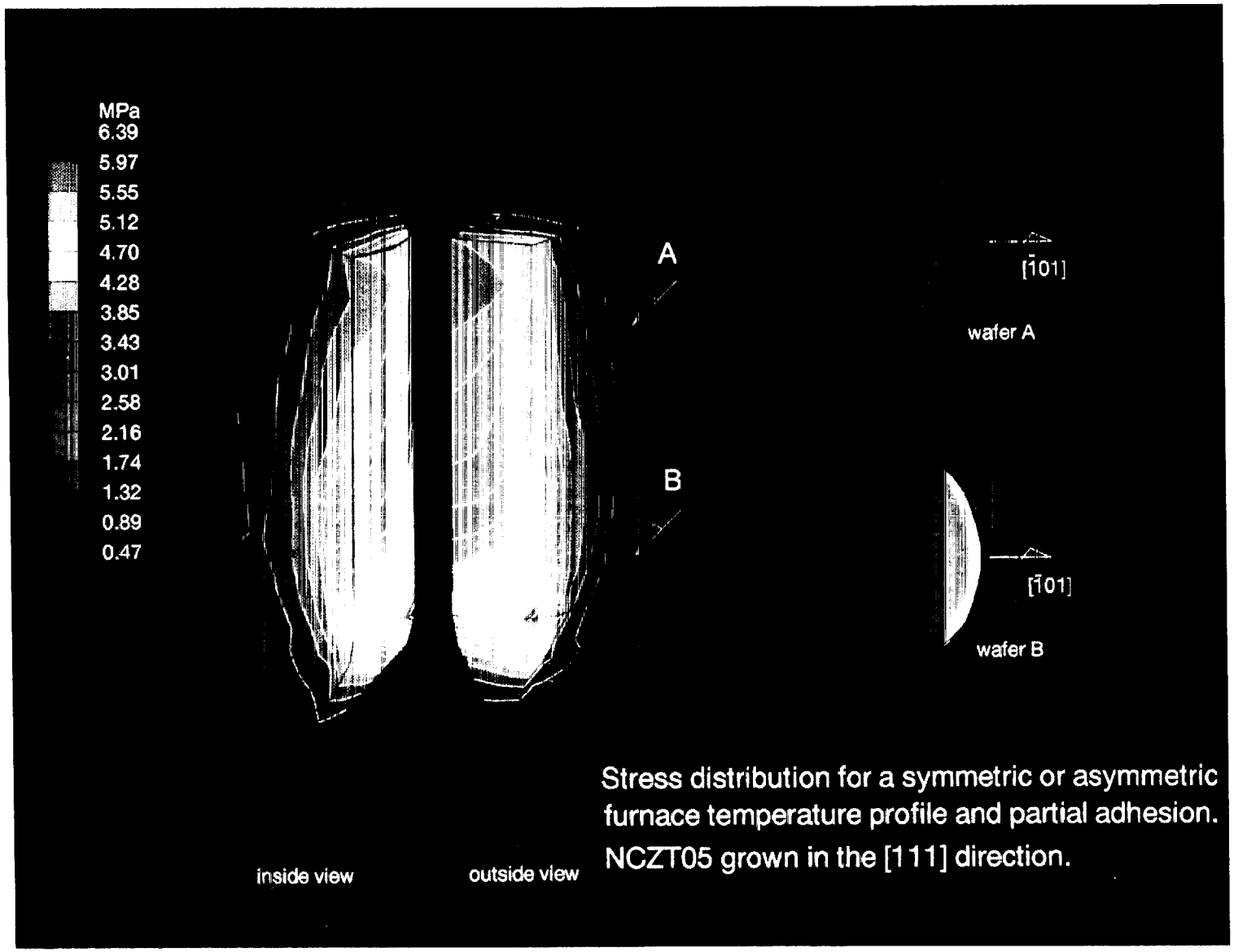

Figure 16 Calculated Stress Distribution for Flight Samples with Partial Wall Contact, Asymmetric Temperature Profile, and No Wall Adhesion.

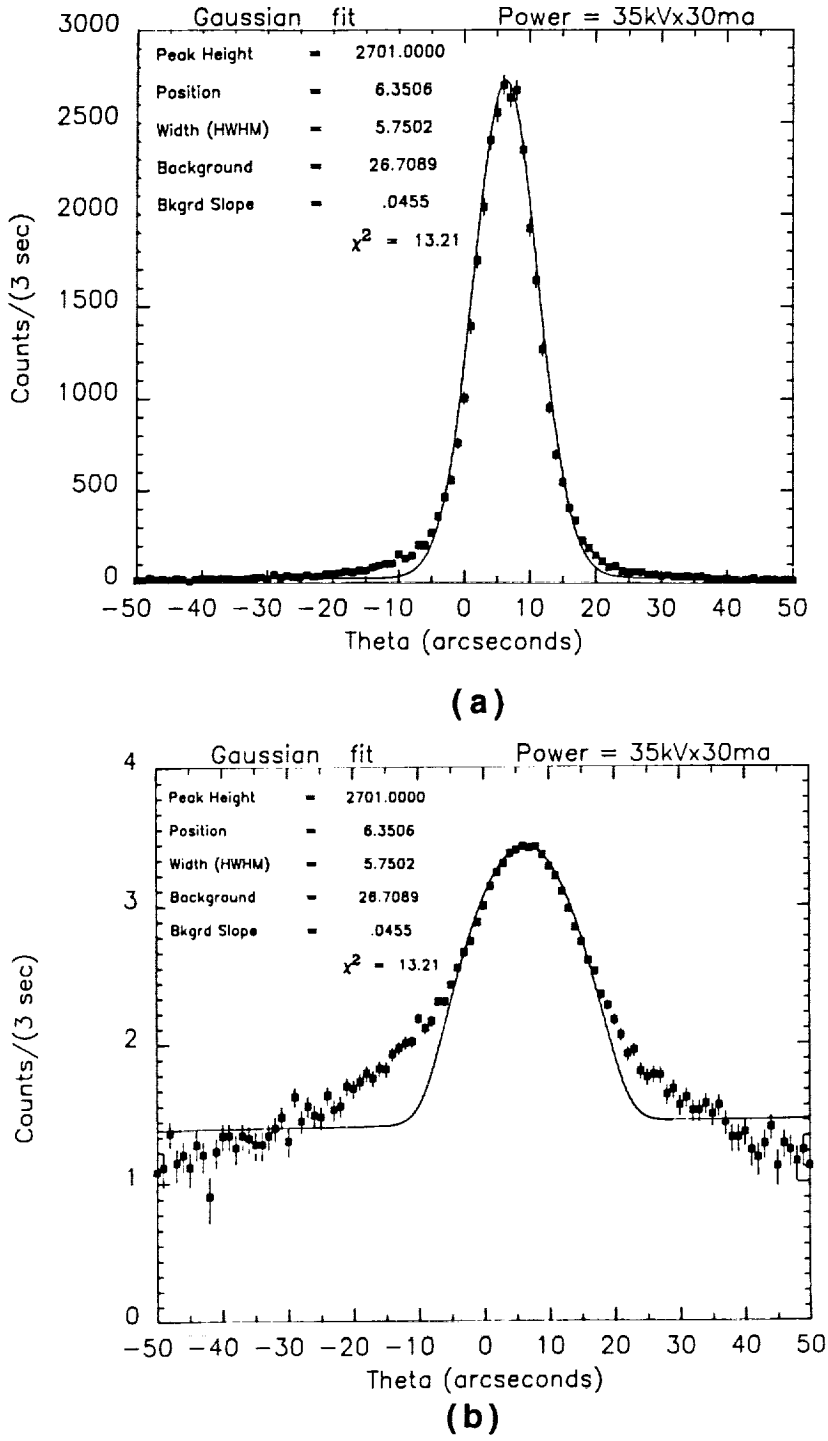

Figure 17 DCRC Curve from PMZF One-g Sample Showing Deviation from Ideal Kinematic Diffraction in the Tails of the Curve, (a) Linear Scale, and (b) Log Scale.

Peak Height	=	48186.6500
Position	=	−5.7064
Width (HWHM)	=	77.2925
Background	=	3934.9880
Bkgrd Slope	=	−10.5792

χ^2 = 21.12

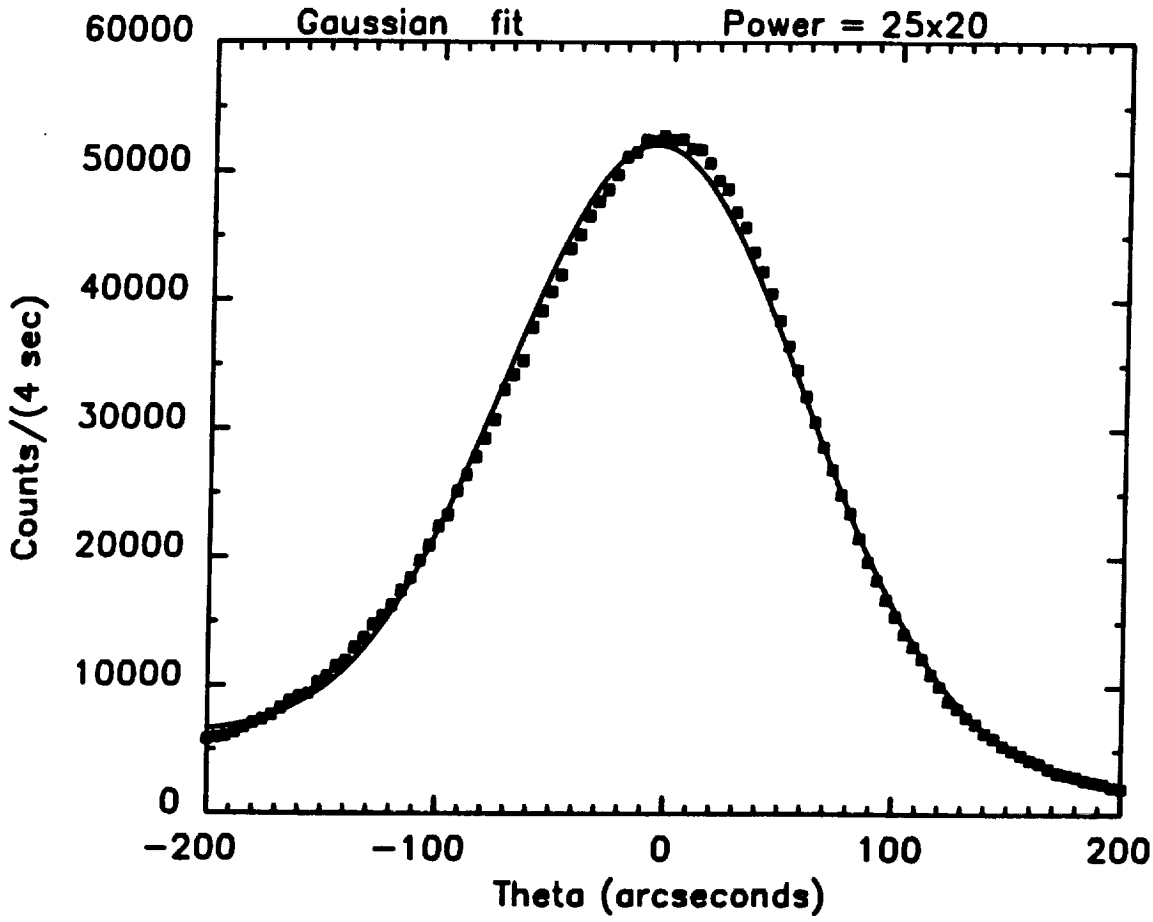

Figure 18 Ideally 'Imperfect' Rocking Curve Peak Described by Kinematic Diffraction Theory.

Peak Height	=	1643.5000	±	.0000
Position	=	−40.7409	±	.1417
Width (HWHM)	=	10.1820	±	.1048
Background	=	13.5773	±	1.6134
Bkgrd Slope	=	−.0326	±	.0385

χ^2 = 2.96

X trans (Millimeter) = 8.2500

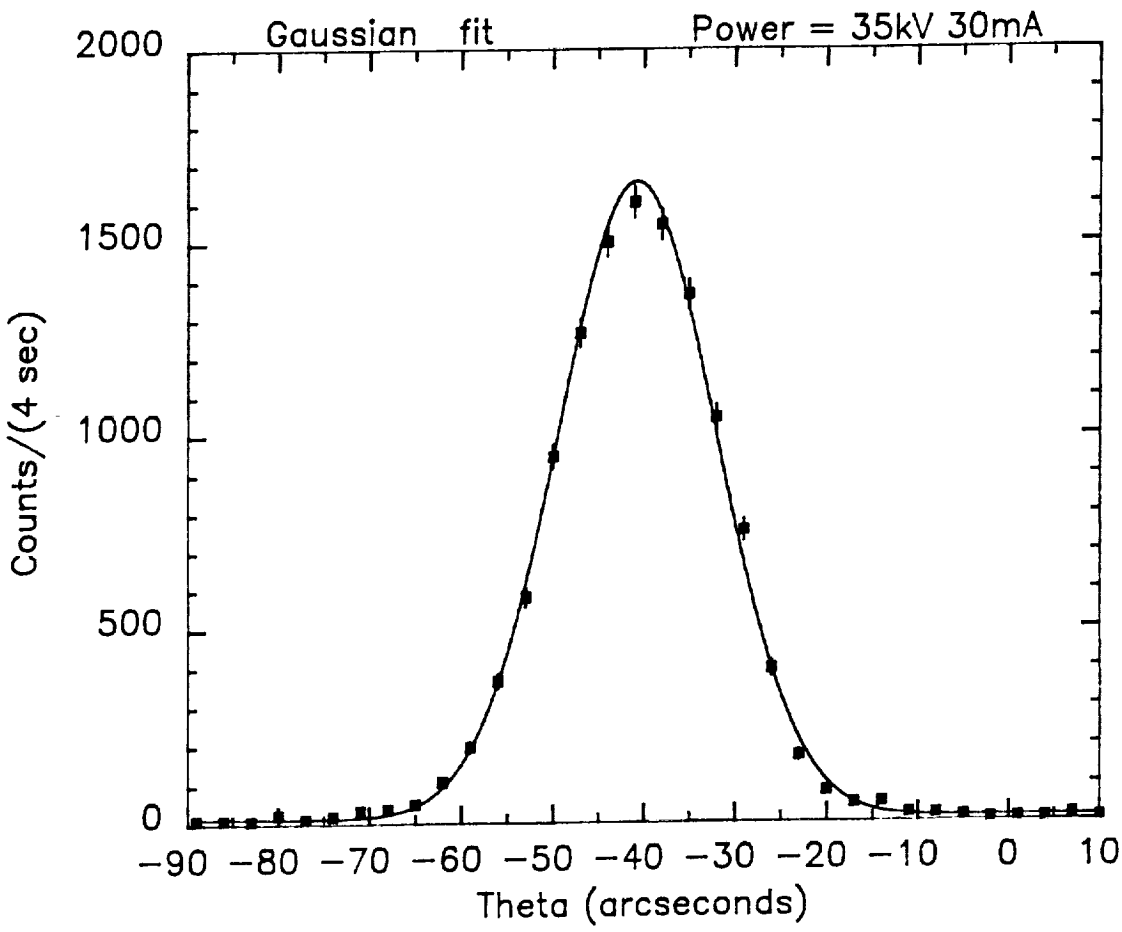

Figure 19 Ideally 'Perfect' Rocking Curve Peak Described by Dynamic Diffraction Theory.

Figure 20 Synchrotron Monochromatic Transmission Topograph Showing an Array of Discrete Dislocations Within the Flight Crystal, GCRC-2.

Discussion

Question: *I wonder if you could make a comment or two about why the mobility dislocations of the flight samples appear to have been lower ?*

Answer: I think it is just a numbers game to the extent that I think the dislocations were mobile, just not many of them are there. That is somewhat surprising. The twin interfaces in general are much lower strain interfaces and have fewer twins in their vicinity at least as these are depicted from an etching standpoint. But I think it is just a numbers game as far as accumulating into, or, migrating into a substructure. You reach a point where even if they migrate, they are not accumulating into a substructure which is on a scale, which we are not used to looking at. It is a rather coarse structure. We can only find one sub-grain or sub-boundary in those wafers that we have imaged so far. It obligated us to map each of the wafers now sequentially so that we can build a three dimensional map of everything that is going on inside of that crystal. That's time consuming. It's only when we finish that and reconstruct that, for instance, we can get a true measure of the radial segregation, a true measure of the dislocation distribution because all of these are oblique sections right now that we are projecting. But to get back to the original question, I think that there are just fewer defects there. They have not accumulated into a substructure that we are used to seeing.

Question: *Is it possible to keep the free surfaces away from the wall container ?*

Answer: To get it away from the wall, basically. We have looked at two geometries. The initial geometry that we have looked at, recent calculations suggest was the wrong geometry to use. Calculations at UAH, if they are correct, suggest that in fact we can have an aspect ratio virtually what we please and that what we should do is perhaps offer additional support for that sample by using a thin liquid encapsulant to keep it away from the wall. I think that is feasible and in fact we will have to talk to the COTR to see if in fact, that is considered within our statement of work, to pursue that concept rather than the taper. The taper that we had measured on the previous flight samples were such that we knew from actual measurements that we could stay from the wall of a taper as low as 8°. It could have put a big burden on the direction of the original g vector; how large the transverse component was; and it placed a lot of burden on the flight dynamics that we felt would not be acceptable. So we are looking for other geometries that would allow us more flexibility and this one looks the best right now.

Question: *Could you comment on the Tellurium motion in the flight sample ?*

Answer: We normally map the Tellurium precipitate. Because of the high cooling rates, even in the standard sample, the Tellurium precipitates are usually quite small. In industry usually there is reference

to two different precipitates. The ones that occur on cooling frequently are referred to as inclusions, which is completely misleading, but that is jargon. These are deadly in the industry because they are typically larger by an order of magnitude and they will frequently generate dislocations around them because of the mismatch and external expansion between that inclusion (one that solidifies and its surrounding solid. It actually precipitates as a liquid). Below the final solidification there is additional precipitation that usually occurs on a sub micro scale. It is very hard to pick up. With respect to the side to side comparison we probably have not done enough of it with regard to infra-red microscopy. I think Don took a look at it. The sample I sent down last week. What we found typically in the previous samples, and the quick look that we have taken of the flight material, is that, the infra-red precipitate size is quite small typically on the order of sub-micron whereas in the slow cooled samples it is typically on the order of 1 to 10 microns. The distribution density I have to go back and look at the numbers, I don't know right off hand what it is.

Question: *I was just wondering there have been some publications done by the Soviets a few years ago where they looked at microscopic surface roughening as a way to try to minimize contact between the melt and the surface and I was wondering if any of that was being looked into and if that would affect your strain density because of the point to point contact ?*

Answer: There has been a lot of work on how to properly contain, if you will, a reactive melt. The roughening of the ampoule inner surfaces is something that has been done frequently and universally on the ground Most commonly in quartz ampoules and basically what it serves to do is to keep at least a portion, as I think Favier described it, of the melt away from the wall at all times. It minimizes the contamination from the wall diffusion of oxygen and silica for instance. We have taken a somewhat different approach in trying to use a nonreactive monolithic inner coating, which is non-wetting, which is in this case graphite or carbon rather. They all have a limitation to the extent that where there is a local failure, and you get contact with the wall, that would be considered a reaction and you get stiction at that wall.